Black Sea Journal of Engineering and Science
doi: 10.34248/bsengineering.1746627

Open Access Journal
e-ISSN: 2619 – 8991

Research Article
Volume 8 - Issue 6: 1739-1747 / November 2025

ASSESSING CLIMATE CHANGE IMPACTS ON PRECIPITATION AND TEMPERATURE IN A MEDITERRANEAN BASIN UNDER CMIP6 SCENARIOS

Emrah YALCIN[1]*, Kübra KOPARAL BOZKURT[1]

[1]*Kırsehir Ahi Evran University, Faculty of Engineering-Architecture, Department of Civil Engineering, 40100, Kırsehir, Türkiye*

Abstract: This study explores projected climate change within a Mediterranean basin, with a particular focus on Ermenek Creek in southern Türkiye. The assessment utilizes precipitation, maximum temperature, and minimum temperature simulations from 24 Global Circulation Models (GCMs) belonging to the latest, sixth phase of the Coupled Model Intercomparison Project (CMIP6) to develop multi-model ensemble (MME) projections under both the CMIP6 historical experiment and two shared socio-economic pathway (SSP) scenarios: the mid-range SSP2-4.5 and the high-end SSP5-8.5. The MMEs are constructed using the best-performing CMIP6 GCMs at the Alanya and Hadim meteorological stations (MSs), which serve as representative synoptic points for the Ermenek watershed. To adequately represent model projection uncertainty, ensemble means are computed for each climate variable using bias-corrected simulations of one to eight models, with the optimal ensemble size determined through a multi-criteria basin-wide performance assessment relative to observed data. Findings reveal that incorporating more than three GCMs yields only peripheral improvements in simulation performance across evaluation metrics. Consequently, climate projections are derived using MMEs composed of the top three performing models and are analyzed over three 25-year periods between the years 2025 and 2099, relative to the historical baseline of 1968-2014. By reaching the end of the century, annual average maximum/minimum temperatures are expected to rise by up to 3.04 °C/2.74 °C at the Alanya MS and 3.34 °C/2.94 °C at the Hadim MS under SSP2-4.5, and by up to 5.21 °C/4.52 °C and 5.98 °C/4.84 °C, respectively, under SSP5-8.5. Concurrently, annual mean daily precipitation is expected to decline by as much as 10.6% and 8.9% at the Alanya and Hadim MSs, respectively, under SSP2-4.5, and by 24.9% and 23.4% under SSP5-8.5.

Keywords: Climate change, CMIP6, Multi-model ensemble, Precipitation, Temperature, Mediterranean hot spot

***Corresponding author:** Kırsehir Ahi Evran University, Faculty of Engineering-Architecture, Department of Civil Engineering, 40100, Kırsehir, Türkiye
E mail: emrah.yalcin@ahievran.edu.tr (E. YALCIN)
Emrah YALCIN https://orcid.org/0000-0002-3742-8866
Kübra KOPARAL BOZKURT https://orcid.org/0000-0002-9836-5133

Received: July 20, 2025
Accepted: September 17, 2025
Published: November 15, 2025

Cite as: Yalcin E, Koparal Bozkurt K. 2025. Assessing climate change impacts on precipitation and temperature in a Mediterranean basin under CMIP6 scenarios. BSJ Eng Sci, 8(6): 1739-1747.

1. Introduction

Effective climate change mitigation and adaptation strategies critically depend on reliable projections derived from climate models (Eyring et al., 2019). Global Circulation Models (GCMs) are the most advanced tools available for simulating large-scale climate dynamics; however, they remain subject to substantial uncertainties stemming from various sources. One major contributor is the unpredictability of future anthropogenic emissions, which introduces variability in projections of greenhouse gases and aerosols—commonly referred to as scenario uncertainty (van Vuuren et al., 2011; Yip et al., 2011). To address this, standardized socio-economic and emissions pathways, such as the representative concentration pathways (RCPs) and the shared socio-economic pathways (SSPs), are employed. Additionally, structural differences among models—due to varied parameterizations, simplifications, and numerical approximations—lead to inter-model discrepancies, further compounding model-related uncertainty (Murphy et al., 2004; Knutti et al., 2019).

The rapid advancement of climate modeling in recent decades has produced an expanding archive of GCMs, with more than 60 models included in the fifth phase of the Coupled Model Intercomparison Project (CMIP5) and over 80 in the latest sixth phase (CMIP6) (Eyring et al., 2019; Wang et al., 2020). While using a large ensemble of GCMs is recommended to capture the full range of model uncertainty (Santer et al., 2009; Knutti et al., 2010), it can be computationally prohibitive—particularly for hydrological impact assessments that require high-resolution simulations. Therefore, identifying an optimal subset of GCMs that balances comprehensiveness with computational feasibility is essential. This requirement is especially pertinent for researchers and practitioners conducting climate-driven hydrological assessments, where model parsimony and computational efficiency must be weighed against scientific rigor.

Multi-model ensembles (MMEs) have become a widely adopted approach for representing uncertainty in climatic and hydrological projections under climate change. However, the question of how many GCMs are sufficient within such ensembles to reliably characterize

this uncertainty remains open. GCM selection strategies generally fall into two categories: performance-based selection, in which models are ranked by their ability to reproduce historical climate observations (Evans et al., 2013; Raju and Kumar, 2014; Ahmadalipour et al., 2017; Yalcin, 2023; Yalcin, 2024), and uncertainty-focused approaches, where models are chosen to preserve the spread of future climate projections (Warszawski et al., 2014; Cannon, 2018). While performance-based rankings offer objectivity, they can be region-specific and time-dependent (Hui et al., 2019), necessitating context-specific evaluations. Conversely, envelope-based selection methods have shown that a limited number of models (e.g., around 10) can sufficiently capture the uncertainty range of hydrological impacts (Wang et al., 2018), supporting the core rationale behind MME applications.

In this context, this study examines the influence of the number of member GCMs on the projection performance of MMEs in climate change assessments, focusing on the Ermenek Creek basin in Türkiye (Figure 1). Climatic changes in the basin are assessed using precipitation and temperature projections for the Alanya and Hadim meteorological stations (MSs), which serve as representative synoptic locations for the watershed. The methodological framework begins with preprocessing daily raw precipitation, maximum temperature, and minimum temperature simulations from 24 GCMs in the CMIP6 database, covering both the CMIP6 historical experiment and the future scenarios SSP2-4.5 and SSP5-8.5 (Eyring et al., 2016; O'Neill et al., 2016). These simulations are then bias-corrected using the linear scaling (LS) method to improve alignment with observed data. Subsequently, the effect of ensemble size on the projection performance of MMEs is evaluated for both precipitation and temperature variables over historical GCM simulations. Based on this evaluation, climate projections are generated using MMEs that demonstrate optimal performance under both historical and future scenarios. Finally, projected climate changes are analyzed across three future 25-year intervals from 2025 to 2099, relative to the historical baseline period of 1968-2014. The methodological structure applied is illustrated in Figure 2. Overall, the study provides a robust framework for generating reliable climate projections, supporting evidence-based planning and adaptation strategies in climate-sensitive regions such as the Mediterranean hot spot.

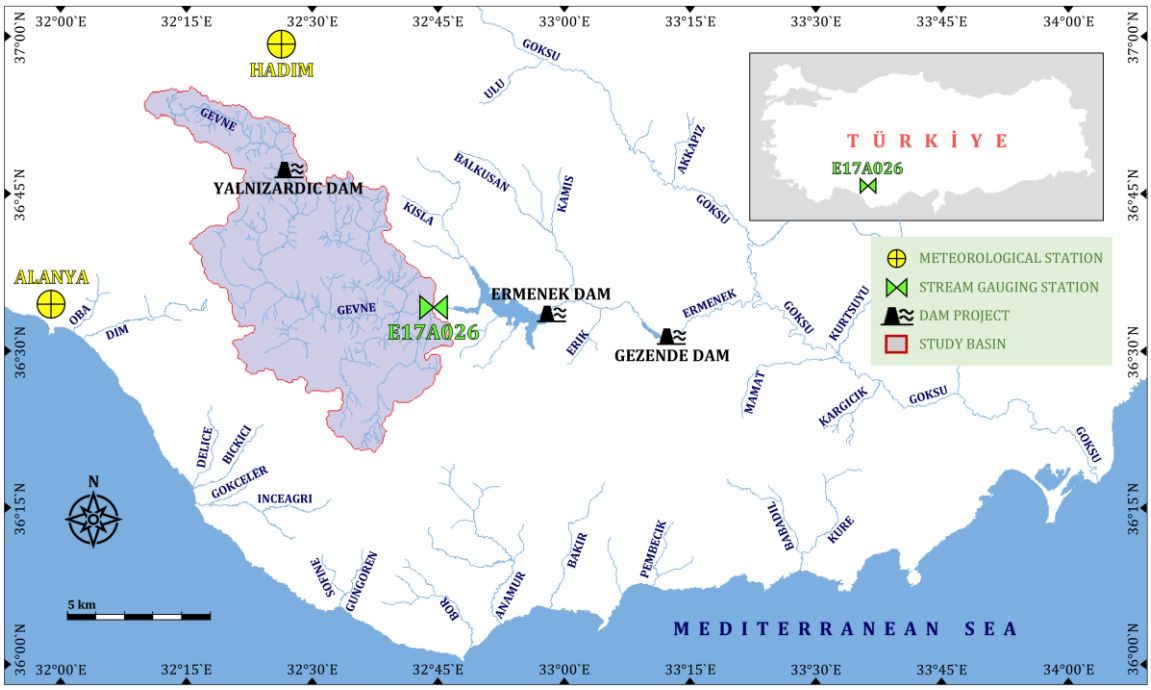

Figure 1. Geographical layout of the study area.

2. Materials and Methods

2.1. Study Area and Meteorological Data

The Mediterranean region (10° W to 40° E, 30° N to 45° N; Iturbide et al., 2020) lies between the hot, arid climate of northern Africa and the cooler, more humid climate of Europe (Cramer et al., 2018). This climatic contrast is partly driven by the influence of nearby oceans, land-sea interactions, and typical mid-latitude atmospheric circulation patterns (Boé and Terray, 2014). Global warming does not affect all regions equally, and according to Giorgi (2006) and Lionello and Scarascia (2018), the Mediterranean is considered a hot spot for climate change. It is therefore crucial for countries bordering the Mediterranean Sea to adapt to evolving climate-related threats (Gleick, 2014; Cramer et al., 2018). These nations face significant challenges due to their complex and varied socio-economic conditions, which increase their vulnerability to climate change and its impacts (Cos et al., 2022). Within this hot spot, the case study is selected from Türkiye, specifically from its Mediterranean region.

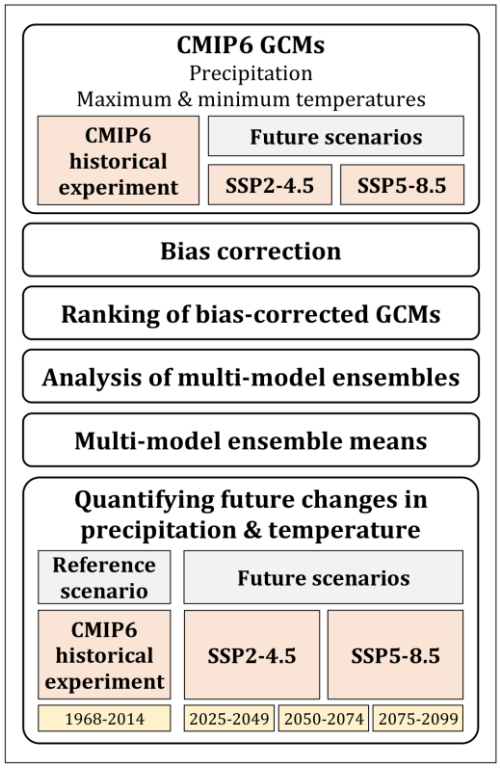

Figure 2. Schematic representation of the applied methodology.

The Göksu River, a major tributary flowing through the Mediterranean region of Türkiye, is 260 km long and, like the Seyhan and Ceyhan rivers—also important water sources in the region—ultimately discharges into the Mediterranean Sea. A major branch of the Göksu River, Ermenek Creek, is selected as the focus of this study. Along Ermenek Creek, from upstream to downstream, there are three hydroelectric power plant (HPP) projects: the Yalnizardic Dam and HPP, the Ermenek Dam and HPP, and the Gezende Dam and HPP (Figure 1). In designing these projects, streamflow measurements from the Yesilkoy stream gauging station (SGS) were used to assess inflow capacities at the dam locations (Yolsu, 2010). Identified by station ID E17A026, the Yesilkoy SGS is situated at an elevation of 662 meters on Ermenek Creek and covers a watershed area of 1,418.4 km^2 (Figure 1) (DSI, 2023).

In-situ weather observations from synoptic MSs near the Yesilkoy SGS watershed are obtained from the Turkish State Meteorological Service (MGM). Among these, the Alanya MS (Station ID: 17310), located at an elevation of 6 meters, and the Hadim MS (Station ID: 17928), located at 1,552 meters, are identified as having the longest and least-interrupted records of precipitation and temperature for the Yesilkoy basin (Figure 1) (MGM, 2023a; MGM, 2023b). The basin coverage ratios of the Alanya and Hadim stations for the Yesilkoy watershed are calculated as 33% and 67%, respectively, based on the constructed Thiessen polygons. According to long-term meteorological statistics, the Alanya MS records an annual mean precipitation of 1,112.7 mm, an annual mean maximum temperature of 23.9 °C, and an annual mean minimum temperature of 15.5 °C. For the Hadim MS, the corresponding values are 663.6 mm, 15.4 °C, and 5.1 °C, respectively (MGM, 2023c; MGM, 2023d).

2.2. GCM Data from CMIP6

Daily datasets of precipitation, maximum temperature, and minimum temperature, simulated by 24 CMIP6 GCMs under the CMIP6 historical experiment and the future scenarios SSP2-4.5 and SSP5-8.5, are sourced from the Earth System Grid Federation (ESGF) portal (ESGF, 2022). The selection of these GCMs is predicated on the availability of daily-resolution simulation outputs and the inclusion of the considered SSP scenarios under the first ensemble member (i.e., r1i1p1f1), thereby ensuring consistency and enabling equitable comparison of model performance (Sun et al., 2022). Table 1 presents the model identifiers and spatial resolutions of the chosen GCMs. To ensure spatial consistency among the models, the climate datasets—originally available at varying grid sizes—are resampled to a standardized 0.5° × 0.5° latitude-longitude grid covering the borders of Türkiye. This resampling employs the first-order conservative remapping technique developed by Jones (1999). All data preprocessing—including merging, manipulation, interpolation, and geographic subsetting—is conducted using the Climate Data Operators (CDO) software developed by the Max Planck Institute for Meteorology (Schulzweida, 2021).

GCM outputs require bias correction to address inherent systematic deviations and ensure alignment with observed climatological characteristics, including distributional properties, temporal sequencing, and magnitude (Tan et al., 2020). Accordingly, GCM datasets extracted for the geographic coordinates of the Alanya and Hadim MSs are bias-adjusted against the respective stations' daily observational records to mitigate potential point-scale systematic biases across both historical and future periods. This correction employs the LS technique, introduced by Lenderink et al. (2007) and implemented via the Climate Model Data for Hydrologic Modelling (CMhyd) platform (Rathjens et al., 2016). The LS method aligns GCM outputs with observed long-term monthly means: daily temperature data are adjusted by adding the mean monthly deviation between observed and simulated values, while daily precipitation is corrected using a monthly scaling factor, thereby preserving observed mean precipitation levels (Mendez et al., 2020).

2.3. Generation of Climate Change Scenarios Using MMEs

To evaluate the historical performance of bias-corrected simulations generated by the 24 GCMs chosen from the CMIP6 database, a comprehensive assessment is conducted for the 1968-2014 period. This historical analysis period is determined based on the observation periods of the synoptic MSs. The performance assessment is carried out on a monthly timescale using four widely recognized performance metrics: the modified index of agreement (md), the normalized root mean square error (nRMSE), the Kling-Gupta efficiency

(KGE), and the fractions skill score (FSS). These metrics collectively enable a robust assessment of the temporal and spatial reliability of the GCM simulations in replicating observed climatological conditions.

Table 1. List of the CMIP6 GCMs considered in this study

GCM	Resolution in Arc Degrees	
	Longitude	Latitude
ACCESS-CM2	1.875	1.25
ACCESS-ESM1-5	1.875	1.25
BCC-CSM2-MR	1.125	1.112-1.121
CanESM5	2.8125	2.767-2.791
CMCC-ESM2	1.25	0.9424084
EC-Earth3	0.703125	0.696-0.702
EC-Earth3-CC	0.703125	0.696-0.702
EC-Earth3-Veg	0.703125	0.696-0.702
EC-Earth3-Veg-LR	1.125	1.112-1.121
FGOALS-g3	2	2.025-5.181
GFDL-CM4	1.25	1
GFDL-ESM4	1.25	1
INM-CM4-8	2	1.5
INM-CM5-0	2	1.5
IPSL-CM6A-LR	2.5	1.267606
KIOST-ESM	1.875	~1.9
MIROC6	1.40625	1.389-1.401
MPI-ESM1-2-HR	0.9375	0.927-0.935
MPI-ESM1-2-LR	1.875	1.850-1.865
MRI-ESM2-0	1.125	1.112-1.121
NESM3	1.875	1.850-1.865
NorESM2-LM	2.5	1.894737
NorESM2-MM	1.25	0.9424084
TaiESM1	1.25	0.9424084

The md metric improves upon the original index of agreement by avoiding the inflation of differences caused by squared error terms and instead applying more appropriate weighting (Legates and McCabe, 1999). The index ranges from 0 (no agreement) to 1 (perfect agreement) and is considered particularly suitable for validating hydrological and hydroclimatic models. The nRMSE provides a dimensionless error metric by normalizing the RMSE with respect to the observed data range (Almeida et al., 2015). Although it can take any positive value, lower values are preferred as they indicate smaller deviations from observations. The KGE, developed by Gupta et al. (2009), is a goodness-of-fit measure that incorporates correlation, variability ratio, and bias ratio. Its values span from $-\infty$ to 1, with values closer to 1 signifying better performance. KGE allows for a more comprehensive evaluation of model behavior by simultaneously capturing multiple performance aspects. The FSS assesses the spatial consistency between simulated and observed data (Roberts and Lean, 2008). Ranging from 0 to 1, values closer to 1 signify higher spatial alignment.

To refine an evaluation at the watershed level, performance metrics calculated at individual MSs are weighted based on the area each station represents within the Yesilkoy SGS watershed. Specifically, metrics from the Hadim MS contribute 67% to the overall performance, while those from the Alanya MS account for the remaining 33%. This area-weighted aggregation ensures a more accurate representation of meteorological conditions over the Yesilkoy watershed. Following the calculation of basin-wide performance metrics for each GCM, the models are ranked using a comprehensive rating metric (RM) as proposed by Chen et al. (2011). For precipitation, RM scores are used directly to select GCMs for ensembling. For temperature (both maximum and minimum), RM scores determined separately for minimum and maximum temperature simulations are combined to generate a unified ranking that represents overall temperature simulation performance.

Recognizing the limitations of relying on a single GCM for climate impact assessments (Wang et al., 2020), this study explores the formation of MMEs using the top-performing GCMs. Despite the lack of consensus in the literature over the optimal number of GCMs, many studies recommend using three to ten models to adequately represent uncertainty (Kim et al., 2016; Bağçaci et al., 2021; Seker and Gumus, 2022; Yalcin, 2023; Yalcin, 2024). In this study, for each climate variable, MME means are computed for ensemble sizes ranging from one to eight using a simple arithmetic averaging approach (Ahmed et al., 2019). The performance of each ensemble configuration is evaluated across the three climate variables using basin-wide md, nRMSE, KGE, and FSS scores.

Based on these evaluations, the optimal ensemble size is selected for future projections of precipitation and temperature in the Yesilkoy SGS watershed under the mid-range SSP2-4.5 and the high-end SSP5-8.5 scenarios. The optimal-performing MME simulations from the 1968-2014 period under the CMIP6 historical experiment provide the baseline climate for evaluating future climatic changes over the watershed. Future projections from the optimal-performing MMEs under the SSP2-4.5 and SSP5-8.5 scenarios are examined over the 2025-2049, 2050-2074, and 2075-2099 periods.

3. Results and Discussion

3.1. Evaluation of MME Performance

Table 2 presents the basin-wide performance rankings of the GCMs, calculated based on the basin coverage ratios of the Alanya and Hadim MSs, for bias-corrected precipitation and temperature simulations under the CMIP6 historical experiment for the 1968-2014 period. Accordingly, the top eight GCMs for precipitation are identified as CanESM5, GFDL-ESM4, MRI-ESM2-0, GFDL-CM4, EC-Earth3-Veg, ACCESS-CM2, EC-Earth3-CC, and EC-Earth3. For maximum and minimum temperatures, the highest-performing GCMs are GFDL-CM4, MRI-ESM2-0, MPI-ESM1-2-HR, BCC-CSM2-MR, TaiESM1, ACCESS-ESM1-5, INM-CM4-8, and EC-Earth3-CC. MMEs

comprising the top-performing one to eight GCMs are used to generate daily time series projections under the CMIP6 historical experiment and the considered SSP scenarios by calculating the arithmetic mean of the bias-corrected outputs from individual GCMs at each station location.

Table 2. Performance-based ranks of the CMIP6 GCMs for the Yesilkoy SGS basin

GCM	Precipitation	Temperature
ACCESS-CM2	6	23
ACCESS-ESM1-5	11	6
BCC-CSM2-MR	18	4
CanESM5	1	18
CMCC-ESM2	10	16
EC-Earth3	8	19
EC-Earth3-CC	7	8
EC-Earth3-Veg	5	22
EC-Earth3-Veg-LR	14	24
FGOALS-g3	15	12
GFDL-CM4	4	1
GFDL-ESM4	2	10
INM-CM4-8	20	7
INM-CM5-0	9	17
IPSL-CM6A-LR	13	14
KIOST-ESM	16	15
MIROC6	17	13
MPI-ESM1-2-HR	12	3
MPI-ESM1-2-LR	23	21
MRI-ESM2-0	3	2
NESM3	24	20
NorESM2-LM	21	11
NorESM2-MM	22	9
TaiESM1	19	5

Figure 3 illustrates the basin-wide performance metrics—md, nRMSE, KGE, and FSS—for MME projections generated using varying numbers of GCM members under the CMIP6 historical experiment, evaluated against observed data from the Alanya and Hadim stations. The evaluation focuses on identifying the optimal ensemble size that yields md, KGE, and FSS values closest to 1 and nRMSE values closest to 0 for both precipitation and temperature variables. The results indicate that using more than three GCMs does not lead to further improvement across the evaluation metrics. In contrast, using only one or two GCMs tends to result in lower performance based on the selected criteria.

For precipitation, the MME—comprising CanESM5, GFDL-ESM4, and MRI-ESM2-0—yields basin-wide performance values of 0.648 for md, 0.109 for nRMSE, 0.582 for KGE, and 0.825 for FSS. For maximum and minimum temperatures, the MME—formed from GFDL-CM4, MRI-ESM2-0, and MPI-ESM1-2-HR—reaches values of 0.895 for md, 0.059 for nRMSE, 0.965 for KGE, and 0.995 for FSS in maximum temperature simulations. In minimum temperature simulations, the same ensemble yields values of 0.883 for md, 0.062 for nRMSE, 0.950 for KGE, and 0.984 for FSS. The performance of precipitation simulations—particularly in terms of md and KGE—appears to be less satisfactory. Figure 3 confirms that this limitation is not attributable to the number of GCMs included in the ensemble. Similar findings are reported in previous studies (Ahmed et al., 2019; Seker and Gumus, 2022; Yalcin, 2024), which applied different bias correction methods and ensemble averaging approaches. These results suggest that GCMs generally perform better in simulating temperature than precipitation.

Nevertheless, for both precipitation and temperature, the MMEs composed of the three best-performing GCMs produce simulations that closely align with observed data from the Alanya and Hadim stations in terms of monthly, seasonal, and annual means under the CMIP6 historical experiment. During the 1968-2014 period, the observed daily average total precipitation values for autumn, winter, spring, summer, and annually are 3.32, 6.56, 2.23, 0.17, and 3.05 mm, respectively, at Alanya, and 2.04, 4.55, 2.39, 0.58, and 2.39 mm at Hadim. For the same period, the corresponding ensemble estimates for Alanya are 3.23, 6.54, 2.15, 0.17, and 3.01 mm, while those for Hadim are 2.02, 4.57, 2.35, 0.56, and 2.37 mm.

Regarding temperature, the observed seasonal and annual average maximum and minimum temperatures during the 1968-2014 period are 26.10 °C and 17.30 °C in autumn, 16.78 °C and 9.14 °C in winter, 21.42 °C and 13.38 °C in spring, 30.85 °C and 22.59 °C in summer, and 23.81 °C and 15.63 °C annually for Alanya. For Hadim, the corresponding values are 16.98 °C and 6.32 °C in autumn, 4.85°C and -3.63 °C in winter, 13.77 °C and 3.58 °C in spring, 25.65 °C and 13.52 °C in summer, and 15.33 °C and 4.96 °C annually. The ensemble simulations for Alanya yield values of 26.14 °C and 16.76 °C in autumn, 16.80 °C and 8.83 °C in winter, 21.34 °C and 12.98 °C in spring, 30.90 °C and 22.15 °C in summer, and 23.82 °C and 15.20 °C annually. For Hadim, the corresponding ensemble estimates are 16.66 °C and 6.33 °C in autumn, 4.90 °C and -3.60 °C in winter, 13.78 °C and 3.67 °C in spring, 25.68 °C and 13.65°C in summer, and 15.28 °C and 5.03 °C annually.

3.2. Projected Changes in Climate

Climate projections generated by the MMEs, composed of the three top-performing GCMs, under the SSP2-4.5 and SSP5-8.5 scenarios are evaluated based on seasonal and annual means for the 2025-2049, 2050-2074, and 2075-2099 periods, using projections attained for the CMIP6 historical experiment across the 1968-2014 period as the reference baseline (Table 3). Under the mid-forcing SSP2-4.5 scenario, the most pronounced decreases in mean annual daily precipitation occur during the 2050-2074 and 2075-2099 intervals. At the Alanya MS, projected reductions reach 7.0% and 10.6%, respectively, while the Hadim MS exhibits corresponding declines of 7.1% and 8.9%. Autumn precipitation at the Alanya MS decreases by 15.0% and 24.8% during the same periods, with the Hadim MS experiencing similar reductions of

15.4% and 25.4%. Meanwhile, summer precipitation at the Hadim MS shows modest increases of 4.5% and 7.9% during 2050-2074 and 2075-2099, respectively. Maximum and minimum temperatures rise consistently across both stations, reaching 3.04 °C and 2.74 °C at the Alanya MS and 3.34 °C and 2.94 °C at the Hadim MS by the last future period.

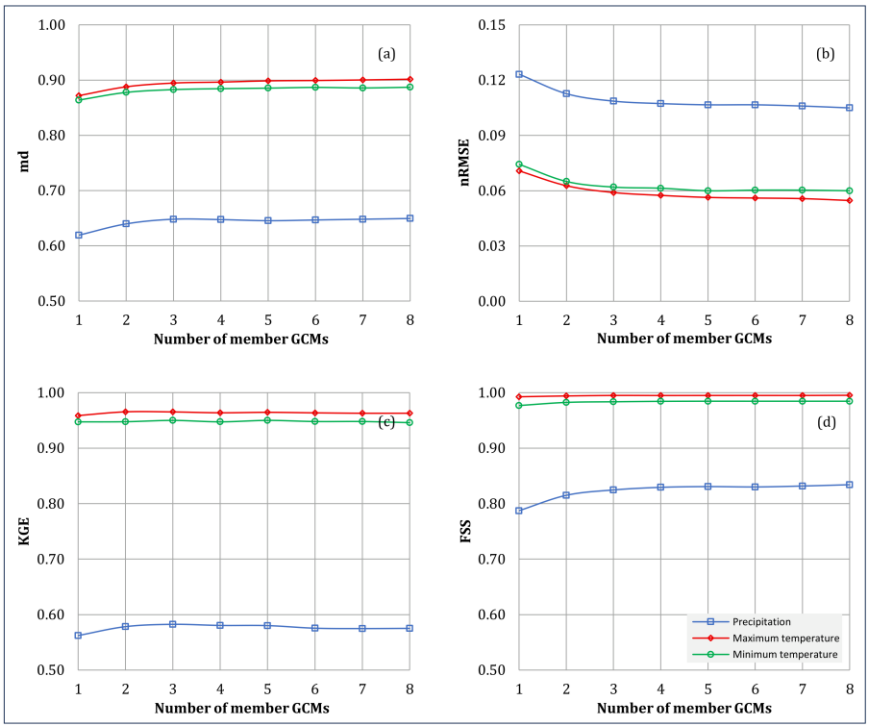

Figure 3. Evaluation of MME performance based on the (a) md, (b) nRMSE, (c) KGE, and (d) FSS indices.

Under the high-end SSP5-8.5 scenario, climate change signals intensify relative to SSP2-4.5 (Table 3). At the Alanya MS, the mean annual daily precipitation decreases by 11.9% and 24.9% for the 2050-2074 and 2075-2099 periods, while the Hadim MS shows similar reductions of 12.0% and 23.4%. Autumn and winter precipitation at the Alanya MS decline by 20.5% and 10.4%, respectively, over the 2050-2074 period, with corresponding decreases of 25.4% and 13.2% projected at the Hadim MS. Additionally, between 2025 and 2049, the Hadim MS experiences a 12.0% reduction in autumn precipitation. Summer precipitation increases at the Hadim MS are also evident under the SSP5-8.5 scenario; nevertheless, the magnitude of this increase diminishes over time—amounting to 8.3%, 3.6%, and 0.5% across the three projection periods. By the last future period, seasonal reductions become more substantial: at the Alanya MS, autumn, winter, and spring precipitation decline by 34.7%, 19.2%, and 28.7%, respectively, while at the Hadim MS, the respective decreases are 36.6%, 21.4%, and 21.3%. In terms of thermal response, maximum and minimum temperatures exhibit steady increases, reaching 5.21°C and 4.52°C at the Alanya MS and 5.98°C and 4.84°C at the Hadim MS by the 2075-2099 period.

4. Conclusion

This study explores the impact of the number of member GCMs on the projection performance of MMEs in climate change analyses, focusing on the Ermenek Creek basin in Türkiye, located within the Mediterranean region—one of the world's prominent climate change hot spots. The analysis shows that MMEs composed of the three best-performing GCMs exhibit robust performance across the evaluated statistical metrics for both precipitation and temperature variables. Furthermore, increasing the number of GCMs beyond three does not yield substantial improvements in projection performance.

MMEs constructed using the top three GCMs for precipitation and temperature are employed to generate projections under the SSP2-4.5 and SSP5-8.5 scenarios for the 2025-2099 period. These projections are compared against simulations from the CMIP6 historical experiment for the 1968-2014 baseline period. The results designate that, by reaching the end of the century, annual average maximum/minimum temperatures at the Alanya and Hadim MSs increase by up to 3.04 °C/2.74 °C and 3.34 °C/2.94 °C, respectively, under the mid-range SSP2-4.5 scenario, and by up to 5.21 °C/4.52 °C and 5.98 °C/4.84 °C, respectively, under the high-end SSP5-8.5 scenario. Additionally, under SSP2-4.5, the annual average daily total precipitation decreases by up to 10.6% and 8.9% at the Alanya and Hadim MSs, respectively, while under SSP5-8.5, these reductions reach 24.9% and 23.4%.

Table 3. Climate projections under the CMIP6 historical experiment, SSP2-4.5, and SSP5-8.5 scenarios

	Scenario		CMIP6 historical experiment	SSP2-4.5			SSP5-8.5		
	(Analysis period)		(1968-2014)	(2025-2049)	(2050-2074)	(2075-2099)	(2025-2049)	(2050-2074)	(2075-2099)
Alanya MS	Precipitation (mm/day)	Autumn	3.23	3.08	2.75	2.43	2.92	2.57	2.11
		Winter	6.54	6.47	6.33	6.17	6.31	5.86	5.29
		Spring	2.15	2.10	2.01	2.04	2.12	2.07	1.53
		Summer	0.17	0.16	0.16	0.16	0.16	0.15	0.15
		Annual	3.01	2.94	2.80	2.69	2.86	2.65	2.26
	Maximum temperature (°C)	Autumn	26.14	27.91	28.64	29.40	28.41	30.15	31.73
		Winter	16.80	18.08	18.76	19.31	18.43	19.76	20.99
		Spring	21.34	22.68	23.44	24.02	22.92	24.48	26.32
		Summer	30.90	33.12	33.92	34.58	33.34	35.18	36.94
		Annual	23.82	25.48	26.22	26.86	25.80	27.42	29.03
	Minimum temperature (°C)	Autumn	16.76	18.43	19.18	19.89	18.89	20.48	21.89
		Winter	8.83	10.02	10.53	11.02	10.27	11.35	12.34
		Spring	12.98	14.18	14.72	15.18	14.30	15.56	16.97
		Summer	22.15	24.23	24.92	25.59	24.39	25.99	27.57
		Annual	15.20	16.74	17.37	17.95	16.99	18.37	19.72
Hadim MS	Precipitation (mm/day)	Autumn	2.02	1.86	1.71	1.51	1.78	1.50	1.28
		Winter	4.57	4.47	4.27	4.26	4.28	3.97	3.59
		Spring	2.35	2.31	2.27	2.30	2.34	2.32	1.85
		Summer	0.56	0.56	0.59	0.61	0.61	0.58	0.57
		Annual	2.37	2.29	2.20	2.16	2.24	2.09	1.82
	Maximum temperature (°C)	Autumn	16.66	18.65	19.36	20.22	19.23	21.22	23.03
		Winter	4.90	6.29	7.00	7.63	6.68	8.20	9.52
		Spring	13.78	15.23	16.05	16.66	15.53	17.32	19.36
		Summer	25.68	28.13	29.07	29.77	28.46	30.69	32.93
		Annual	15.28	17.12	17.92	18.62	17.52	19.41	21.26
	Minimum temperature (°C)	Autumn	6.33	8.15	8.98	9.75	8.64	10.38	11.92
		Winter	-3.60	-2.38	-1.88	-1.38	-2.13	-1.08	-0.21
		Spring	3.67	4.88	5.41	5.85	4.96	6.26	7.67
		Summer	13.65	15.94	16.79	17.49	16.10	17.99	19.94
		Annual	5.03	6.68	7.36	7.97	6.93	8.43	9.87

Future studies should focus on investigating alternative bias correction methods and ensemble averaging techniques for GCM datasets in the establishment of MMEs, with the objective of improving the alignment of projected precipitation with observed station data (Kim et al., 2016; Wang et al., 2020). Furthermore, upcoming assessments of climate change impacts should prioritize the use of simulations derived from CMIP6-based regional climate models, which are anticipated to be more accessible in the near future. Additionally, the current analytical framework could be further refined by incorporating projected changes in other key climatic variables, including wind, humidity, and solar radiation (Gorguner and Kavvas, 2020).

Author Contributions

The percentages of the authors' contributions are presented below. All authors reviewed and approved the final version of the manuscript.

	E.Y.	K.K.B.
C	70	30
D	70	30
S	100	-
DCP	60	40
DAI	70	30
L	70	30
W	70	30
CR	70	30
SR	70	30
PM	100	-
FA	100	-

C=Concept, D= design, S= supervision, DCP= data collection and/or processing, DAI= data analysis and/or interpretation, L= literature search, W= writing, CR= critical review, SR= submission and revision, PM= project management, FA= funding acquisition.

Conflict of Interest

The authors declared that there is no conflict of interest.

Ethical Consideration

Ethics committee approval was not required for this study because of there was no study on animals or humans.

References

Ahmadalipour A, Rana A, Moradkhani H, Sharma A. 2017. Multi-criteria evaluation of CMIP5 GCMs for climate change impact analysis. Theor Appl Climatol, 128: 71-87.

Ahmed K, Sachindra DA, Shahid S, Demirel MC, Chung E-S. 2019. Selection of multi-model ensemble of general circulation models for the simulation of precipitation and maximum and minimum temperature based on spatial assessment metrics. Hydrol Earth Syst Sci, 23(11): 4803-4824.

Almeida MP, Perpiñán O, Narvarte L. 2015. PV power forecast using a nonparametric PV model. Sol Energy, 115: 354-368.

Bağçaci SÇ, Yucel I, Duzenli E, Yilmaz MT. 2021. Intercomparison of the expected change in the temperature and the precipitation retrieved from CMIP6 and CMIP5 climate projections: a Mediterranean hot spot case, Türkiye. Atmos Res, 256: 105576.

Boé J, Terray L. 2014. Land-sea contrast, soil-atmosphere and cloud-temperature interactions: interplays and roles in future summer European climate change. Clim Dyn, 42(3): 683-699.

Cannon AJ. 2018. Multivariate quantile mapping bias correction: an N-dimensional probability density function transform for climate model simulations of multiple variables. Clim Dyn, 50: 31-49.

Chen W, Jiang Z, Li L. 2011. Probabilistic projections of climate change over China under the SRES A1B scenario using 28 AOGCMs. J Climate, 24: 4741-4756.

Cos J, Doblas-Reyes F, Jury M, Marcos R, Bretonnière P-A, Samsó M. 2022. The Mediterranean climate change hotspot in the CMIP5 and CMIP6 projections. Earth Syst Dynam, 13(1): 321-340.

Cramer W, Guiot J, Fader M, Garrabou J, Gattuso J-P, Iglesias A, Lange MA, Lionello P, Llasat MC, Paz S, Peñuelas J, Snoussi M, Toreti A, Tsimplis MN, Xoplaki E. 2018. Climate change and interconnected risks to sustainable development in the Mediterranean. Nature Clim Change, 8: 972-980.

DSI. 2023. General Directorate of State Hydraulic Works: Flow gauging yearbooks (1959-2015). General Directorate of State Hydraulic Works, Ankara, Türkiye.

ESGF. 2022. Earth System Grid Federation: WCRP Coupled Model Intercomparison Project (Phase 6). URL: https://esgf-node.llnl.gov/projects/cmip6/ (accessed date: May 15, 2022).

Evans JP, Ji F, Abramowitz G, Ekström M. 2013. Optimally choosing small ensemble members to produce robust climate simulations. Environ Res Lett, 8: 044050.

Eyring V, Bony S, Meehl GA, Senior CA, Stevens B, Stouffer RJ, Taylor KE. 2016. Overview of the Coupled Model Intercomparison Project Phase 6 (CMIP6) experimental design and organization. Geosci Model Dev, 9:1937-1958.

Eyring V, Cox PM, Flato GM, Gleckler PJ, Abramowitz G, Caldwell P, Collins WD, Gier BK, Hall AD, Hoffman FM, Hurtt GC, Jahn A, Jones CD, Klein SA, Krasting JP, Kwiatkowski L, Lorenz R, Maloney E, Meehl GA, Pendergrass AG, Pincus R, Ruane AC, Russell JL, Sanderson BM, Santer BD, Sherwood SC, Simpson IR, Stouffer RJ, Williamson MS. 2019. Taking climate model evaluation to the next level. Nat Clim Change, 9: 102-110.

Giorgi F. 2006. Climate change hot-spots. Geophys Res Lett, 33(8): L08707.

Gleick PH. 2014. Water, drought, climate change, and conflict in Syria. Weather Clim Soc, 6(3): 331-340.

Gorguner M, Kavvas ML. 2020. Modeling impacts of future climate change on reservoir storages and irrigation water demands in a Mediterranean basin. Sci Total Environ, 748: 141246.

Gupta HV, Kling H, Yilmaz KK, Martinez GF. 2009. Decomposition of the mean squared error and NSE performance criteria: implications for improving hydrological modelling. J Hydrol, 377(1-2): 80-91.

Hui Y, Chen J, Xu C-Y, Xiong L, Chen H. 2019. Bias nonstationarity of global climate model outputs: the role of internal climate variability and climate model sensitivity. Int J Climatol, 39(4): 2278-2294.

Iturbide M, Gutiérrez JM, Alves LM, Bedia J, Cerezo-Mota R, Cimadevilla E, Cofiño AS, Di Luca A, Faria SH, Gorodetskaya IV, Hauser M, Herrera S, Hennessy K, Hewitt HT, Jones RG, Krakovska S, Manzanas R, Martínez-Castro D, Narisma GT, Nurhati IS, Pinto I, Seneviratne SI, van den Hurk B, Vera CS. 2020. An update of IPCC climate reference regions for subcontinental analysis of climate model data: definition and aggregated datasets. Earth Syst Sci Data, 12(4): 2959-2970.

Jones PW. 1999. First- and second-order conservative remapping schemes for grids in spherical coordinates. Mon Weather Rev, 127(9): 2204-2210.

Kim J, Ivanov VY, Fatichi S. 2016. Climate change and uncertainty assessment over a hydroclimatic transect of Michigan. Stoch Environ Res Risk Assess, 30(3): 923-944.

Knutti R, Baumberger C, Hirsch Hadorn G. 2019. Uncertainty quantification using multiple models - prospects and challenges. In: Beisbart C, Saam NJ, editors. Computer simulation validation: fundamental concepts, methodological frameworks, and philosophical perspectives. Springer, Cham, Switzerland, pp: 835-855.

Knutti R, Furrer R, Tebaldi C, Cermak J, Meehl GA. 2010. Challenges in combining projections from multiple climate models. J Clim, 23: 2739-2758.

Legates DR, McCabe GJ. 1999. Evaluating the use of "goodness-of-fit" measures in hydrologic and hydroclimatic model validation. Water Resour Res, 35(1): 233-241.

Lenderink G, Buishand A, van Deursen W. 2007. Estimates of future discharges of the river Rhine using two scenario methodologies: direct versus delta approach. Hydrol Earth Syst Sci, 11: 1145-1159.

Lionello P, Scarascia L. 2018. The relation between climate change in the Mediterranean region and global warming. Reg Environ Change, 18: 1481-1493.

Mendez M, Maathuis B, Hein-Griggs D, Alvarado-Gamboa L-F. 2020. Performance evaluation of bias correction methods for climate change monthly precipitation projections over Costa Rica. Water, 12(2): 482.

MGM. 2023a. Turkish State Meteorological Service: Daily precipitation, maximum temperature, and minimum temperature records of the Alanya meteorological station (Station ID: 17310). Turkish State Meteorol Service, Ankara, Türkiye.

MGM. 2023b. Turkish State Meteorological Service: Daily precipitation, maximum temperature, and minimum temperature records of the Hadim meteorological station (Station ID: 17928). Turkish State Meteorol Service, Ankara, Türkiye.

MGM. 2023c. Turkish State Meteorological Service: Long-term all parameters bulletin for the Alanya meteorological station (Station ID: 17310). Turkish State Meteorol Service, Ankara, Türkiye.

MGM. 2023d. Turkish State Meteorological Service: Long-term all parameters bulletin for the Hadim meteorological station (Station ID: 17928). Turkish State Meteorol Service, Ankara, Türkiye.

Murphy JM, Sexton DMH, Barnett DN, Jones GS, Webb MJ, Collins M, Stainforth DA. 2004. Quantification of modeling uncertainties in a large ensemble of climate change simulations. Nature, 430: 768-772.

O'Neill BC, Tebaldi C, van Vuuren DP, Eyring V, Friedlingstein P, Hurtt G, Knutti R, Kriegler E, Lamarque J-F, Lowe J, Meehl GA, Moss R, Riahi K, Sanderson BM. 2016. The Scenario Model Intercomparison Project (ScenarioMIP) for CMIP6. Geosci Model Dev, 9: 3461-3482.

Raju KS, Kumar DN. 2014. Ranking of global climate models for India using multicriterion analysis. Clim Res, 60: 103-117.

Rathjens H, Bieger K, Srinivasan R, Chaubey I, Arnold JG. 2016. CMhyd user manual: documentation for preparing simulated climate change data for hydrologic impact studies. URL: https://swat.tamu.edu/media/115265/bias_cor_man.pdf (accessed date: May 25, 2022).

Roberts NM, Lean HW. 2008. Scale-selective verification of rainfall accumulations from high-resolution forecasts of convective events. Mon Weather Rev, 136(1): 78-97.

Santer BD, Taylor KE, Gleckler PJ, Bonfils C, Barnett TP, Pierce DW, Wigley TML, Mears C, Wentz FJ, Brüggemann W, Gillett NP, Klein SA, Solomon S, Stott PA, Wehner MF. 2009. Incorporating model quality information in climate change detection and attribution studies. P Natl Acad Sci USA, 106: 14778-14783.

Schulzweida U. 2021. CDO user guide version 2.0.5. Max Planck Institute for Meteorology, Hamburg, Germany, pp: 2-5.

Seker M, Gumus V. 2022. Projection of temperature and precipitation in the Mediterranean region through multi-model ensemble from CMIP6. Atmos Res, 280:106440.

Sun C, Zhu L, Liu Y, Wei T, Guo Z. 2022. CMIP6 model simulation of concurrent continental warming holes in Eurasia and North America since 1990 and their relation to the Indo-Pacific SST warming. Global Planet Change, 213: 103824.

Tan ML, Juneng L, Tangang FT, Samat N, Chan NW, Yusop Z, Ngai ST. 2020. SouthEast Asia HydrO-meteorological droughT (SEA-HOT) framework: a case study in the Kelantan River Basin, Malaysia. Atmos Res, 246: 105155.

van Vuuren DP, Edmonds J, Kainuma M, Riahi K, Thomson A, Hibbard K, Hurtt GC, Kram T, Krey V, Lamarque J-F, Masui T, Meinshausen M, Nakicenovic N, Smith SJ, Rose SK. 2011. The representative concentration pathways: an overview. Clim Change, 109: 5-31.

Wang H-M, Chen J, Cannon AJ, Xu C-Y, Chen H. 2018. Transferability of climate simulation uncertainty to hydrological impacts. Hydrol Earth Syst Sci, 22: 3739-3759.

Wang H-M, Chen J, Xu C-Y, Zhang J, Chen H. 2020. A framework to quantify the uncertainty contribution of GCMs over multiple sources in hydrological impacts of climate change. Earths Future, 8: e2020EF001602.

Warszawski L, Frieler K, Huber V, Piontek F, Serdeczny O, Schewe J. 2014. The Inter-Sectoral Impact Model Intercomparison Project (ISI-MIP): project framework. P Natl Acad Sci, 111(9): 3228-3232.

Yalcin E. 2023. Quantifying climate change impacts on hydropower production under CMIP6 multi-model ensemble projections using SWAT model. Hydrolog Sci J, 68: 1915-1936.

Yalcin E. 2024. A CMIP6 multi-model ensemble-based analysis of potential climate change impacts on irrigation water demand and supply using SWAT and CROPWAT models: a case study of Akmese Dam, Türkiye. Theor Appl Climatol, 155: 679-699.

Yip S, Ferro CAT, Stephenson DB, Hawkins E. 2011. A simple, coherent framework for partitioning uncertainty in climate predictions. J Clim, 24: 4634-4643.

Yolsu. 2010. Yalnizardic Hydroelectric Power Plant revised feasibility report. Yolsu Engineering Services Limited Company, Ankara, Türkiye, pp: 1-7.